Mesoporous silica synthesized from natural local kaolinas an effective adsorbent for removing of Acid Red 337 and its application in the treatment of real industrial textile effluent

Ibtissem Slatni & Fatima Zohra Elberrichi & Joëlle Duplay & Nor El Houda Fardjaoui & Abdelkrim Guendouzi & Oukacha Guendouzi & Brahim Gasmi & Feryal Akbal & Ilhem Rekkab

Abstract

This paper presents a synthesis of mesoporous silica (MS) from natural clay as a silica source using Pluronic L35 (EO11PO16EO11) as a structure-directing agent. The prepared material was characterized by XRD, X-ray fluorescence, thermogravimetric analysis, SEM, TEM, and N2 adsorption-desorption analyses. Then, mesoporous material was used for the removal of Acid Red 337 (AR337) from aqueous solution, and the treatment of real textile effluent. The effect of pH, contact time, weight of adsorbent, and initial concentration was studied in batch adsorption. The synthesized mesoporous material showed good discoloration efficiency with a 62% percentage. Experiment with real textile wastewater showed that 39%, 40%, and 31.5% of the color, TOC, and chemical oxygen demand respectively were eliminated by using 1 g of MS per liter of wastewater.

Keywords Mesoporous silica (MS) · Adsorption · Acid Red 337 · Real textile effluent

Introduction

In recent years, research on ordered mesoporous silica–based materials has become a major area of interest (Li et al. 2016; Sheng et al. 2017; Zhao et al. 2016), due to their high specific surface area, and uniform pore size distribution and the impor- tant potential applications of mesoporous materials in cataly- sis (Baskaran et al. 2014), adsorption (Chaudhuri et al. 2016; Sheng et al. 2017; Tsai et al. 2015), and wastewater treatment (Chaudhuri et al. 2015).

Typically, the mesoporous silica is prepared with tetramethyl orthosilicate (TMOS) or tetraethyl orthosilicate (TEOS) as silica sources (Bhuiyan et al. 2013; Tsai et al. 2015) using a cooperative surfactant templating. Many minerals rich in SiO_2 or Al_2O_3 have been used as an alternative to silica source. Several studies refer to the use of raw silica sources in ordered mesoporous materials synthesis (Zhou et al. 2013), such as SBA-15 from natural clay (Zhang et al. 2015), MCM-41 from kaolin (Du and Yang 2012; Li et al. 2010), mesoporous silica materials from natural sands (Sheng et al. 2017), natural halloysite (Zhou et al. 2013), and kaolin (Qoniah et al. 2015).

For several years, great effort has been made to study textile effluent treatment and dye removal, in particular. Textile dyeing industry is one of the most chemically intensive indus- tries in the world and known to be one of the main sources of environmental pollution. It uses a variety of chemicals: dyes,

surfactants, solvents, oxidizing agents, reducing agents, synthetic resins, and many other chemical auxiliaries. In addition, a large quantity of water is consumed during the production process. Approximately 200 L of water is required to produce 1 kg of textile (Ghaly et al. 2014). Subsequently, large quantities of effluents are generated, which are rich in color, COD (chemical oxygen demand) complex chemicals, inorganic salts, total dissolved solids (TDS), pH, temperature, turbidity, and salinity (Verma et al. 2012).

Direct discharge of textile wastewater into freshwater gives an undesirable color that reduces sunlight penetration and resists photochemical and biological attacks to aquatic life. Traditional textile wastewater treatment technologies include various combinations of biological, physical, and chemical methods (Ghaly et al. 2014). However, the adsorption method is a very promising technique because of its simplicity and economy and the availability of a wide range of adsorbents (Aguayo-Villarreal et al. 2014; Khan et al. 2015; Khattri and Singh 2009).

Over the past few years, several experiments have been carried out using low-cost natural materials as a silica source such as sawdust (Khattri and Singh 2009), active carbon (Ahmed 2016; Ahmad and Hameed 2009; Bui et al. 2019; Yang et al. 2008), and clay soil (Santos et al. 2015; Yan et al. 2015); they were successfully used to remove toxic dyes from aqueous solutions. A large compilation of potentially effective adsorbents in dye removal can be found in a review of (Yagub et al. 2014). Nevertheless, studies on the adsorption of real textile wastewater remain relatively scarce (Guesh et al. 2016).

This study aims to present a novel synthesized mesoporous silica material using clay from northeastern Algeria and to investigate the ability of this material to remove Acid Red 337 and treat real textile wastewaters by adsorption.

Materials and methods

Materials

Natural kaolin clay (DD3) was used as a silica source for the synthesis of mesoporous silica material.

It was extracted from the Djbal Dbagh mountains, located in Guelma province, Algeria, and is composed of halloysite and kaolinite (halloysite to kaolinite weight ratio of 1.23) (Fardjaoui et al. 2017; Mellouk et al. 2009). Acid Red 337 was purchased from Alfa Kimya (textile chemical company in Istanbul, Turkey) with the commercial name Telon Red FRL (Table 1). Pluronic L35 (EO11-PO08-EO11, MW = 1900) and sodium hydroxide (NaOH 97%) were purchased from Sigma-Aldrich, and hydrochloric acid (HCl 37%) was obtained from Riedel-de Haën. The real textile wastewaters were supplied by COTITEX (a factory specialized in the manufacture of military fabrics in Algeria). During the manufacturing and dyeing processes, two types of dyes (vat and disperse) and different types of chemical substances were used, such as peroxide, caustic soda, and auxiliary products.

Table 1 Main properties of Acid Red 337 dye

Generic name	Acid Red 337
Chemical name (IUPAC)	Sodium 6-amino-4-hydroxy-5-[[2(trifluoromethyl)phenyl]azo] Naphthalene-2-sulfonate
Molecular formula	$C_{17}H_{11}F_3N_3NaO_4S$
Molar mass	433.337 g/mol
λ_{max}	500 nm
CAS number	12270-02-9
Molecular structure in 3D presentation	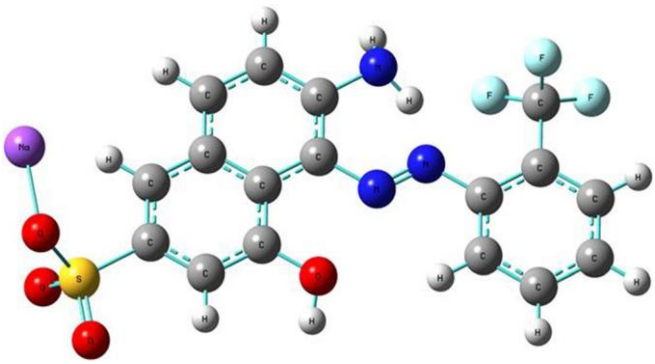

Table 2 Chemical composition of natural kaolin DD3 and synthesized mesoporous silica (wt. %)

Samples	SiO_2	MgO	Al_2O_3	P_2O_5	SO_3	K_2O	CaO	TiO_2	LOI
DD3	41.74	0.017	31.21	0.03	0.313	0.085	0.420	0.017	25.04
MS	89.3	0.015	0.51	0.003	0.045	0.017	0.01	0.006	8.28

LOI (loss on ignition) at 1000 C

Synthesis

Raw natural kaolin (DD3) was calcined at 500 °C for 4 h at a rate of 2 °C/min. Then, 10 g of calcined clay was mixed with 200 mL of 6-M HCl and stirred for 4 h at 80 °C after the solution was filtered, washed with deionized water, and dried at ambient temperature. Mesoporous material was synthesized according to the literature procedure (Zhao et al. 2016), using Pluronic L35 and natural kaolin (DD3) as a silica source, 4 g of Pluronic L35 dissolved in 6.67 g of deionized water and 0.24 g HCl, while stirring at 40 °C. Then, 8.54 g of treated kaolin (DD3) was added to the stirring solution.

These mixtures were stirred continuously for 24 h. The white gel was observed and was transferred to a Teflon-coated autoclave and heated to 100 °C for 48 h. The solid product was separated by filtration and washed several times with deionized water, then dried at room temperature and calcined for 4 h at 500 °C at a rate of 2 °C/min to remove the template L35 and obtain the synthetic mesoporous silica (MS).

Material characterization

The chemical composition of materials was determined by Bruker AXS: SRS 3400 and S8 TIGER X-ray fluorescence (FRX) spectrometer. MS was structurally characterized by the X-ray powder diffraction (XRD) method using Bruker D8 Advance diffractometer under copper Kα radiation (λ = 1.5406 Å) at 40 kV/30 mA, with a scanning rate of 0.08° min^{-1} over 2θ-range between 1° and 10°.

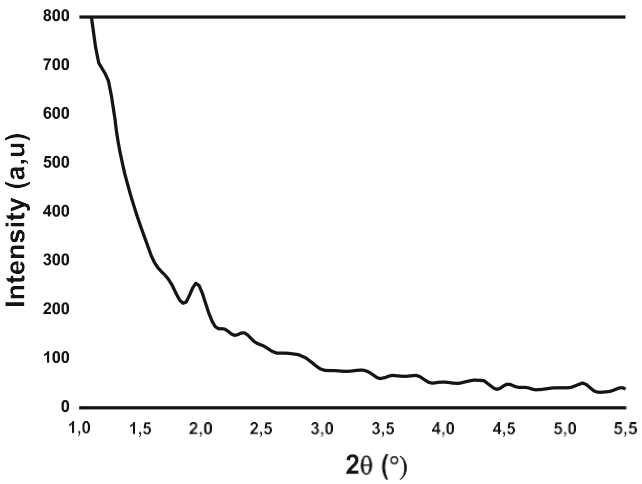

Fig. 1 SXRD pattern of as-synthesized mesoporous silica

Morphological and microstructure analyses were carried out using a Quanta 650 scanning electron microscope (SEM) and JEOL 2100F transmission electron microscopy (TEM) operating at 200 kV and equipped with a probe aberration corrector, an EELS (Gatan Tridiem) spectrometer and an EDXSDD detector.

Nitrogen adsorption-desorption experiments were measured at − 196 °C on a Micromeritics Quantachrome NOVA 1000. The sample was outgassed for 1 h at 100 °C. The surface area was measured according to the Brunauer-Emmett-Teller (BET) method. The average pore size was determined from the N_2 adsorption branch of nitrogen isotherms using the Barrett-Joyner-Halenda (BJH) method. The accuracy of the device given on each surface parameter is as follows: specific surface area (SBET), ± 0.01 m^2/g; pore size, ± 0.35 nm; pore volume, ± 0.001 cm^3/g.

TG analysis of the sample was performed on a DTG-60 instrument in an alumina pan at a 10 °C/min heating rate from 20 to 1000 °C under N_2 flow.

Analytical analysis

Effluent conductivity and pH were determined by the Thermo Scientific Orion Star A215 pH/conductivity benchtop meter. pH measurement is in accordance with ISO 10523 2008. Chemical oxygen demand (COD, mg O_2/L) was carried out as per standard procedures (APHA 1998).

Total organic carbon (TOC) was measured by a Lotix TOC Combustion analyzer (NCASI Method 71.01 1999).

Dye adsorption experiments

Firstly, the Acid Red 337 stock dye solution at 200 mg/L was prepared. Then, the pH effect on the ability of mesoporous silica (MS) to adsorb Acid Red (AR 337) dye was examined in the range of 2–10 (Thue et al. 2018). pH was adjusted to the desired value with 1-M NaOH or HCl before adding the quantity of adsorbent.

Batch adsorption was performed with 200 mL of dye solution at a concentration of C_0 = 100 mg/L and a weighed quantity of m = 0.4 g of MS. The mixture was stirred at room temperature at a speed of r = 300 rpm for 24 h until it reached equilibrium. The solution was then separated from the adsorbent by centrifugation for 15 min at 5000 rpm.

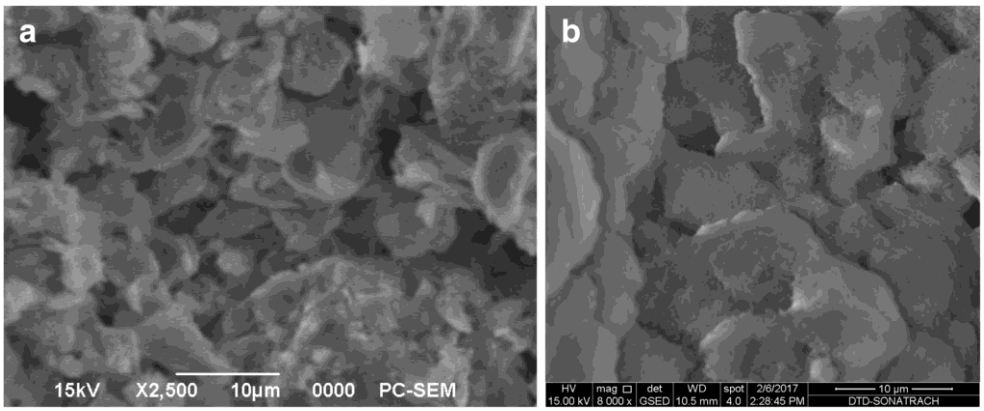

Fig. 2 SEM microphotographs of DD3 kaolin (a) and as-synthesized mesoporous silica MS (b)

Non-adsorbed dye in the final liquid phase was determined by a UV-Vis spectrophotometer at a maximum absorbance wavelength of 500 nm. The quantity (mg) of dye adsorbed per gram of adsorbent was assessed (Q_t), and the highest equilibrium values were used to define the maximum adsorption capacity (Q_{max}) and at equilibrium (Q_e). Q_t and Q_e (mg/g) were calculated using Eqs. (1) and (2):

$$Q_t = \frac{(C_0 - C_t) \times V}{m} \quad (1)$$

$$Q_e = \frac{(C_0 - C_e) \times V}{m} \quad (2)$$

where C_0 and C_e (mg/L) are the liquid-phase concentrations of the adsorbate at the initial time and at equilibrium, respectively, V (L) is the solution volume, and m (g) is the adsorbent mass. To calculate the decolorization efficiency (percentage of removal %R), Eq. (3) was used:

$$\%R = \left(\frac{C_0 - C_t}{C_0}\right) \times 100 \quad (3)$$

Results and discussion

Chemical analysis

The chemical composition of natural kaolin (DD3) and synthesized mesoporous silica (MS) obtained by XRF are shown in Table 2. Results showed that after the treatment of DD3 and synthesis of mesoporous silica, the content of all elements decreased except for SiO_2. This increased from 41.74 to 89.3%.

XRD analysis

The mesoporous silica structure was characterized by small-angle X-ray diffraction (SXRD), as shown in Fig. 1. The pattern shows a small single diffraction peak at $2\theta = 2°$ with smaller intensity, and the absence of the long-range second and third peaks indicates a formation of disordered mesoporous structure (Pan et al. 2013; Zhang et al. 2012, 2014) which is similar to that of mesoporous silica synthesized by sodium

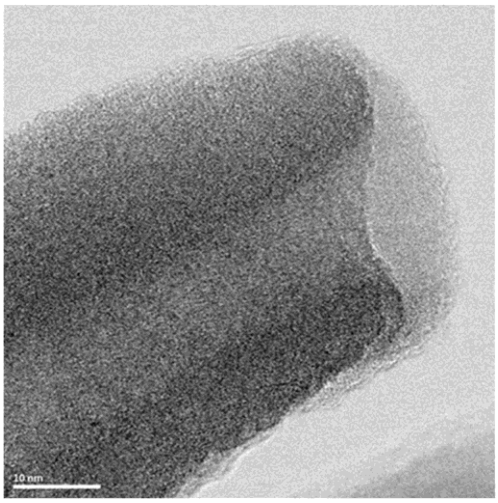

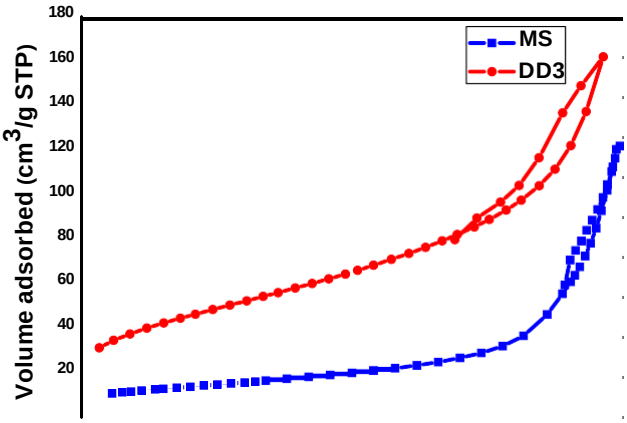

Fig. 3 TEM image of as-synthesized mesoporous silica

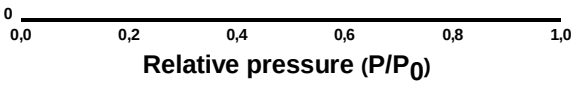

Fig. 4 N2 adsorption-desorption isotherms of DD3 kaolin and as-synthesized mesoporous silica (MS)

Table 3 Surface properties of DD3 kaolin and as-synthesized mesoporous silica (MS)

Sample	BET surface area (m^2/g)	Average pore diameter (nm)	Total pore volume (cm^3/g)
DD3 kaolin	49	2.25	0.20
MS	161	3.06	0.25

silicate as a precursor (Pang and Tang 2005) and the inferior structural order in the SBA-15 sample prepared using bottom ash (Chen et al. 2010). Tanev and Pinnavaia (1996) found that Cn+ surfactant chain with $n < 14$ afforded X-ray amorphous or very poorly ordered products.

SEM and TEM analysis

SEM microphotographs of as-synthesized mesoporous material showed a platy particle shape (Fig. 2b). Similar morphology was found by Li et al. (2015) and Madhusoodana et al. (2006). DD3 kaolin agglomerated structures with small particle size were seen in the corresponding microphotography (Fig. 2a). However, the particle size range for MS is about 25 μm and 8 μm for DD3 kaolin.

TEM analysis results showed no obvious order in pore arrangement, and morphological form is less uniform overall which confirmed the disordered structure of mesoporous material as shown in Fig. 3.

Porosity measurement

Figure 4 illustrates the N_2 adsorption/desorption isotherm of DD3 kaolin and as-synthesized MS. The isotherm shapes of the two samples are different. Based on IUPAC classification (Sing et al. 1985), MS isotherm exhibits a typical type IV class with an H3-type hysteresis loop due to capillary condensation processes which is a characteristic of mesoporous material and indicative of narrow slit-shaped pores similar results have been founded by Auta and Hameed (2012) and Li et al. (2015).

Figure 4 shows for MS, at low relative pressures, a slow increase of nitrogen corresponding to monolayer-multilayer adsorption on the pore walls. At intermediate relative pressures, a sharp step indicative of capillary condensation within mesopores. In the last stage, at high relative pressures, a final plate with a slight inclination associated with multilayer adsorption on the external surface of the particles with pronounced capillary condensation due to framework-confined mesoporous structure (Chen et al. 2010).

The original kaolin had a mixture of types II and IV sorption and a hysteresis loop of H1, which is typical of large-pore microporous solids. Therefore, the size distribution and pore shape of the as-synthesized MS are irregular. The BET specific surface area, pore width, and total pore volume of as-synthesized MS and natural kaolin DD3 are presented in Table 3. The table shows that the mesopores have a diameter of 3.06 nm with a pore volume of 0.250 cm^3/g and a specific surface area of 161 m^2/g. The large increase of prepared silica mesoporous compared with the DD3 kaolin is due to the formation of template mesopores by the added L35 which was assembled with the dissolved silica species of natural kaolin DD3.

A position shift of the capillary condensation toward higher relative pressures indicates the increase of the mesopore size (Kim et al. 2005).

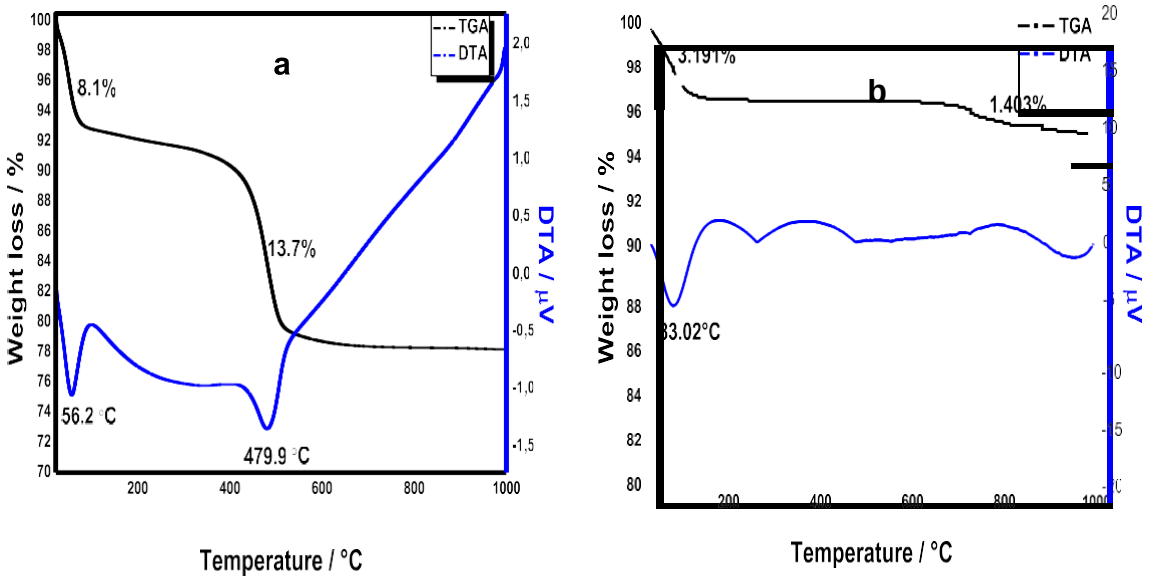

Fig. 5 TGA and DTA curves of a natural kaolin (DD3) and b as-synthesized mesoporous silica

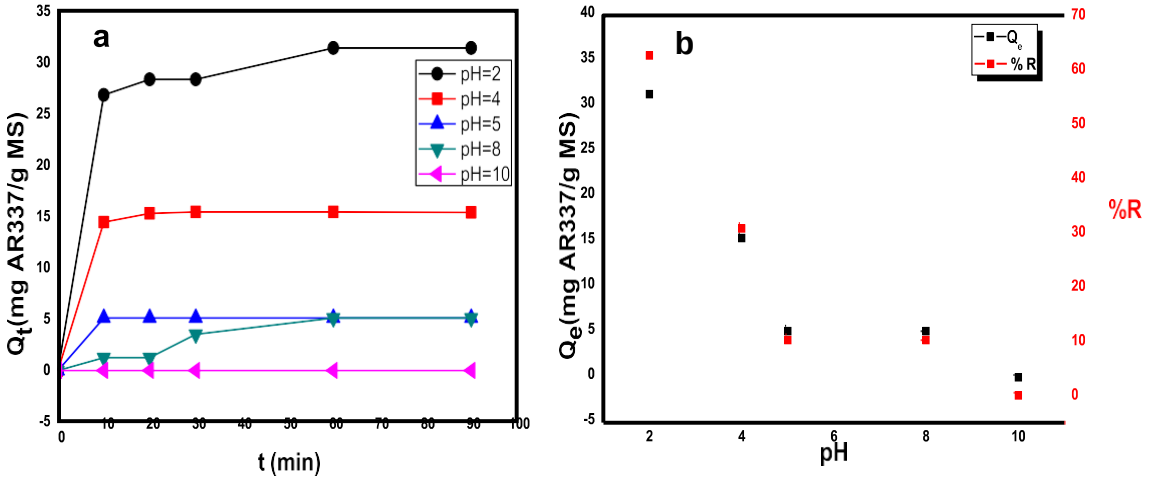

Fig. 6 Effect of pH on Acid Red 337 a adsorption capacity (Q_t) and b %R over synthesized mesoporous silica (C_0 = 100 mg/L, V = 200 mL, T = 20 °C, r = 300 rpm, m = 0.4 g)

Thermal analysis

The evaluation of the product thermal stability by thermogravimetric analysis (TGA) weight curve and differential thermal analysis (DTA) of natural kaolin (DD3) and synthesized MS, is presented in Fig. 5a and b.

It can be noted that natural kaolin DD3 has a mass loss of 8.1% at a temperature of 56.2 °C (Fig. 5a), which implies a loss of moisture. DTA result also shows an endothermic peak at approximately 479 °C corresponding to the second weight loss (13.7%) and is attributed to the external halloysite hydroxylation (Frost and Vassallo 1996).

For synthesized MS (Fig. 5b), it can be observed that a very small weight loss (3.19%) at less than 80 °C accompanied by an endothermic DTA peak corresponds to the loss of free water and a second weight loss of 1.4% between 600 and 1000 °C is attributed to a loss of water due to silanol condensation (Mureseanu et al. 2011). It can therefore be deduced that the synthesized MS has good thermal stability.

Adsorption experiments

Effect of initial solution pH

The solution pH is an important parameter that dominates the adsorption of dyes on adsorbents (Eftekhari et al. 2010). pH can affect the surface charge of the adsorbent and the ionization degree of adsorbate functional groups (Elmoubarki et al. 2015; Thue et al. 2018). Figure 6 shows the equilibrium

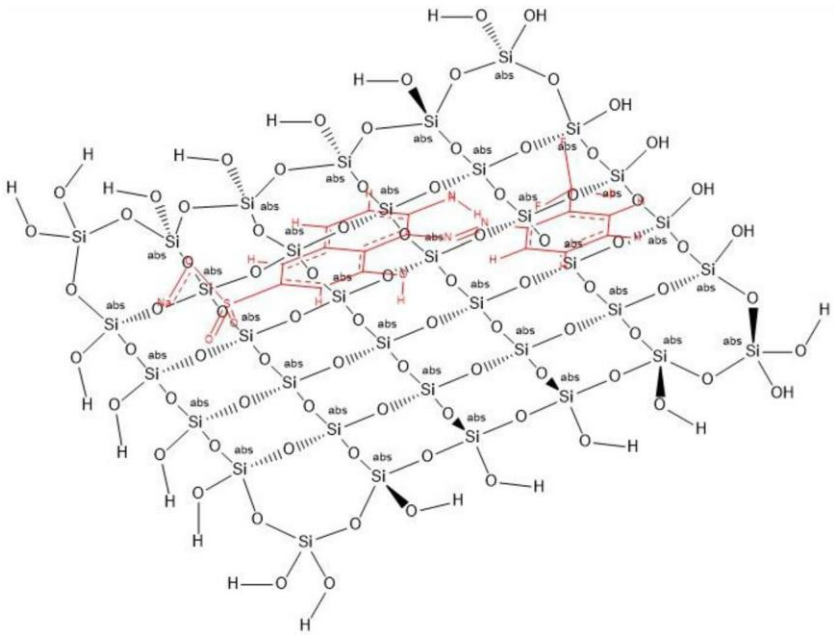

Fig. 7 Adsorption mechanism for Acid Red 337 dye using synthesized mesoporous silica

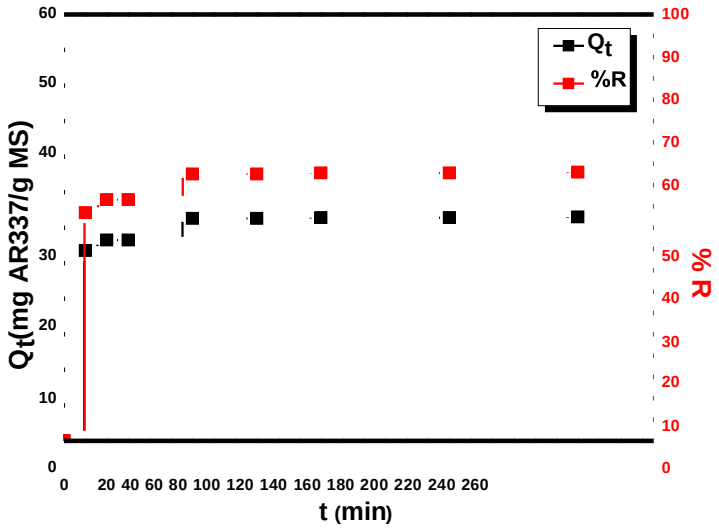

Fig. 8 Effect of contact time (t) on the Acid Red 337 adsorption capacity (Q_t) and %R over the synthesized mesoporous silica (C_0 = 100 mg/L, V = 200 mL, T = 25 °C, r = 300 rpm, pH = 2, m = 0.4 g)

capacities of Acid Red 337 over MS with different pH values, ranging from 2 to 10, for C_0 = 100 mg/L and an adsorbent dose = 2.0 g/L. pH 2 was the ideal condition for Acid Red 337 adsorption on MS, which was used for all further adsorption studies; a similar trend was found by Atrous et al. (2019) in the adsorption of Acid Red 1 and Acid Green 25 on grafted clay and Georgin et al. (2019) for the adsorption of Acid Red 97 on *Beauveria bassiana* spore waste.

In addition, it has been found that by increasing the initial pH in the range of 2–10, the %R decreases from 62.61 to 0% (Fig. 6b), because the charge of the MS becomes larger at lower pH values and smaller at higher pH. The expansion of the adsorption limit at pH 2 can also be attributed to the isoelectric point (*pI)* of mesoporous silica adsorbents that is around 2.5–3 (Gómez et al. 2014). It can be seen that the adsorption capacity increases at lower pH, which indicated that the electrostatic interaction is not the dominant factor adsorption. However, the value kept almost constant between pH 5 and pH 8. The PKa value of Acid Red is between 4 and 5, and then it exists as a cationic form in pH ≤ PKa. At pH acid, the cationic form of the AR 337 is in favor of adsorption. Thus, the mechanism of AR 337 adsorption onto MS should be an electrostatic process. On the other hand, the AR 337 dye changes to an ionic form with increasing pH value and the interaction between the dye and the surface of MS could be explained by H bonding between nitrogen, fluorine, oxygen, and sulfur atoms. In this context, a reaction mechanism is proposed in Fig. 7.

Effect of contact time (t)

Figure 8 illustrates the impact of contact time on AR 337 adsorption over synthesized MS.

Figure 8 also shows that dye adsorption is quick; it reached %R = 56 after 20 min and increased with additional contact time. Equilibrium was achieved at t = 60 min and Q_e =

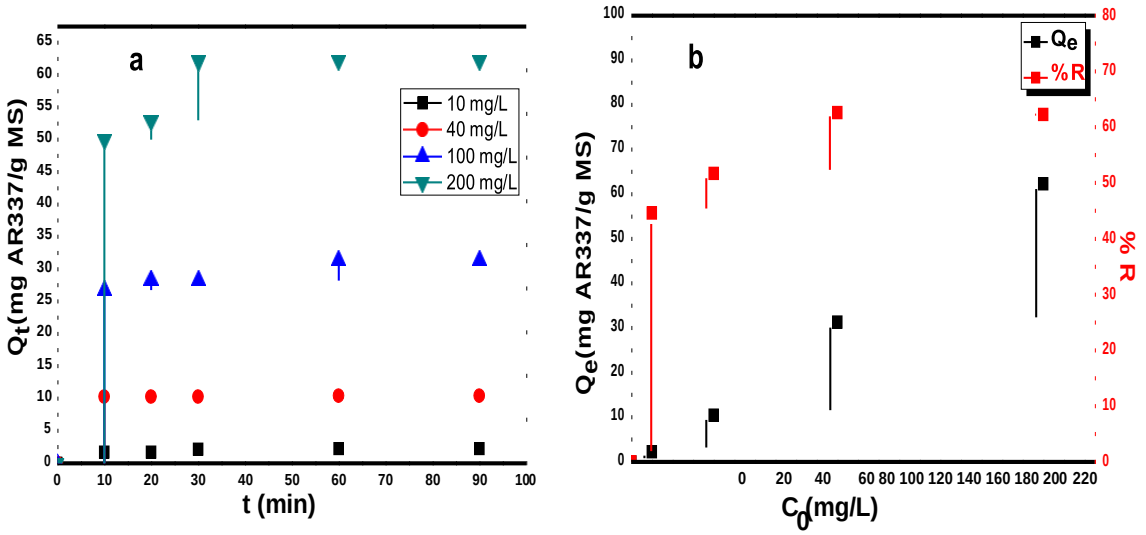

Fig. 9 Effect of initial dye concentration (C_0) on a adsorption capacity (Q_t) and b %R over the as-synthesized mesoporous silica (m = 0.4 g, V = 200 mL, T = 20 °C, r = 300 rpm, pH = 2)

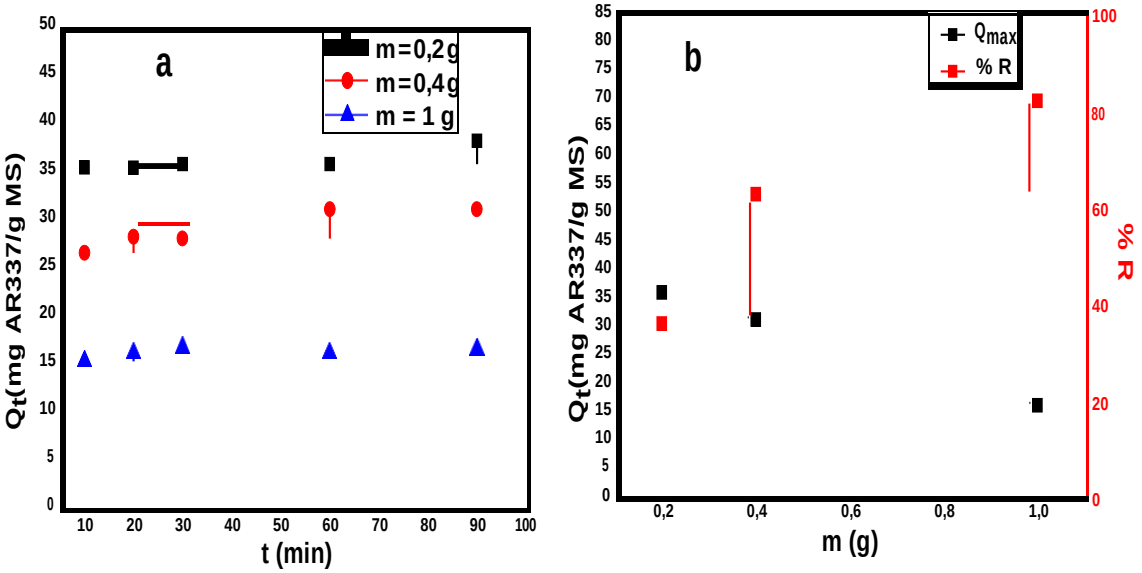

Fig. 10 Effect of adsorbent amount (m) on a the adsorption capacity (Q_t) and b %R over the synthesized mesoporous silica (C_0 = 100 mg/L, V = 200 mL, T = 20 °C, r = 300 rpm, pH = 2)

31.3 mg/g since no change in adsorption capacity was observed (the study was extended to 1440 min). The optimal contact time was 60 min.

Dye concentration effect

To examine the impact of anionic dye fixation on the limit of adsorption onto MS, several tests were performed by modifying the initial concentration of the dye between 10 and 200 mg/L (Fig. 9).

Figure 9 shows that the increase in the initial Acid Red concentration leads to an increase in adsorption capacities (Q_{max} = 62 mg/g). Furthermore, the rate of adsorption is fast and the equilibrium is reached in 10 min for all concentrations and 30 min for C_0 = 200 mg/L. Thus, it indicates the availability for AR337 of accessible active sites on synthesized mesoporous silica (Acisli et al. 2016). The continuous curves showed the monolayer coverage on the adsorbent surface (Khattri and Singh 2009).

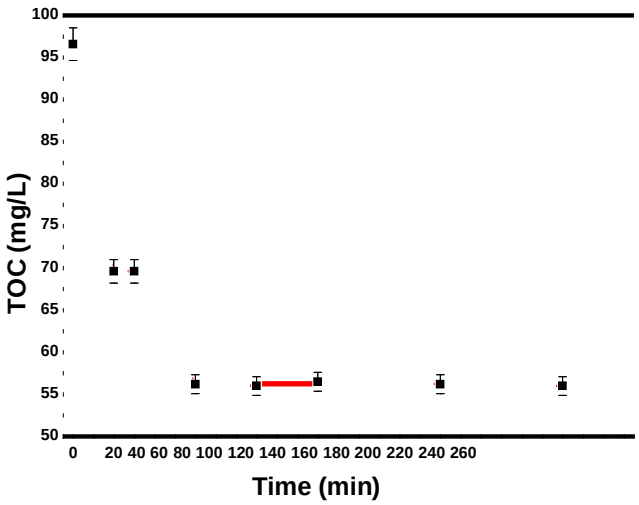

Fig. 11 Effect of treatment time on the reduction of TOC of the real textile effluent by adsorption on as-synthesized mesoporous silica (T = 30 °C, pH = 8.15, m = 1 g, V = 100 mL effluent, r = 300 rpm)

Adsorbent concentration effect

To optimize the amount of the adsorbent, experiments were performed using different quantities of synthesized mesoporous silica (0.2, 0.4, and 1 g/200 mL). Figure 10 illustrates that an increase in the amount of MS from 0.2 to 1 g leads to a decrease in Q_{max} values from 36 to 16.34 mg/g. This can be related to particle interactions, such as aggregation which would result in a decrease in the total surface area of the adsorbent (Acisli et al. 2016). Particle interactions may also cause desorption of a portion of the sorbate that is loosely and reversibly bound to the surface (Shukla et al. 2002). As a result, 0.2 g/200 mL of MS is the optimal amount of mesoporous silica necessary to remove dye at a 100-mg/L concentration.

Use of synthesized mesoporous silica in the treatment of real industrial textile effluent

The potential use of synthesized MS in the treatment of real textile effluent and its ability to reduce color, COD, and TOC were tested. Initial color, COD, and TOC of the sample were 67 Pt-Co, 330 mg/L, and 96.6 mg/L respectively and its pH was 8.15.

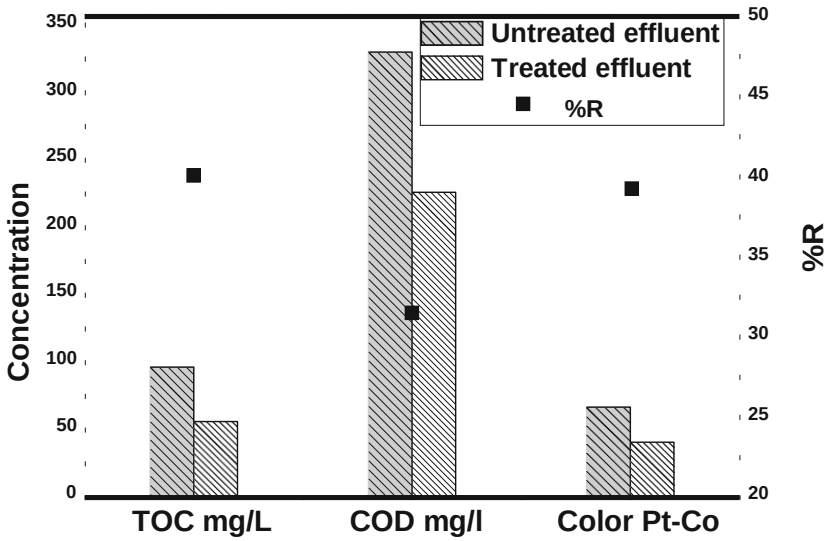

Fig. 12 Percentage of removal and comparison of the concentrations of TOC, COD, and color in untreated and treated wastewater

For this experiment, the textile wastewater was first filtered, and then the batch experiment was conducted in a 250-mL flask containing 100 mL of textile effluent and 0.1 g of adsorbent at room temperature at an average shaker's speed of 300 rpm without changing the pH of the effluent. The mixture was then stirred overnight to reach equilibrium.

Effect of contact time

Figure 11 shows the effect of contact time on the reduction of TOC concentration of the wastewater effluent.

It can be observed that during the first 60 min, there is a fast decrease in TOC concentration. The equilibrium is reached after 1 h of contact time. At first, the solute molecules were adsorbed by the external surface of adsorbent particles, so the adsorption rate was fast. When the adsorption of the external surface reached saturation, the molecules needed to diffuse through the pores of the adsorbent into the internal surface of the particle. This phenomenon may have taken a relatively long contact time (Ahmad and Hameed 2009). A 60-min time period was then used as contact time for color and COD treatment.

TOC, COD, and color removal

Figure 12 provides the concentration reduction and the removal percentage of TOC, COD, and color of wastewater by adsorption on MS.

After adsorption, it can be seen that the concentration of TOC, COD, and color decrease by 40% (from 96.6 to 56 mg/L), 31% (from 330 to 226.25 mg/L), and 39% (from 67 to 41 Pt-Co) respectively. These average values can be explained by the complexity of real effluent chemical composition.

Table 4 lists the comparison of the maximum percentage of COD removed by various adsorbents. The MS synthesized in this work showed a relatively good percentage of COD removal, despite a small specific surface as compared with some previous works reported in the literature.

Theoretical approach of the mechanism of the Acid Red 337 dye adsorption onto mesoporous silica

In order to identify the mechanism of adsorption of the Acid Red 337 dye on to mesoporous silica (MS), at the first step, the

Table 4 Comparison of the maximum percentage of COD removal by various adsorbents

Adsorbent types	S_{BET} (m^2/g)	Dose (g/L)	pH	Contact time (min)	COD removal	References
This work	161	1	8	60	31.5%	/
Activated carbon fiber	1842	0.70	8	50	45.83%	Aber and Sheydaei (2012)
Composite material zeolite/N-doped porous activated carbon	1240	0.5	/	3 h	68%	Xin et al. (2019)
Bamboo-based activated carbon (BAC)	988.23	3	3	10 h	75%	Ahmad and Hameed (2009)

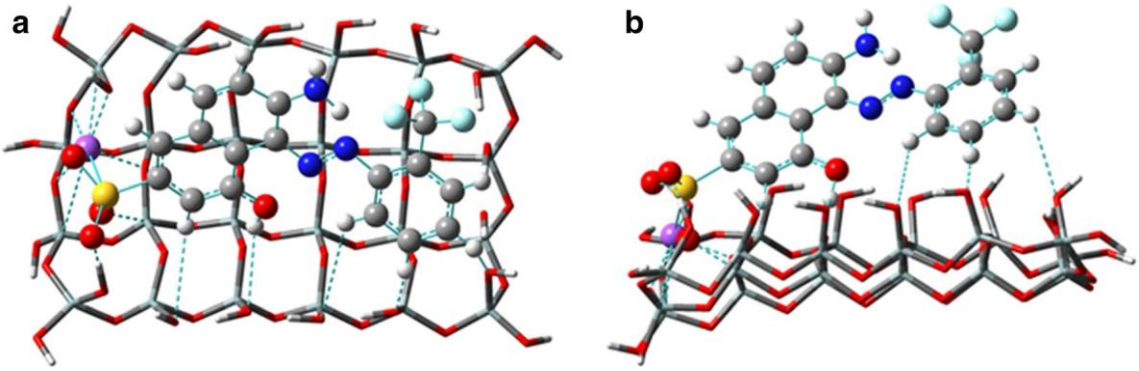

Fig. 13 Schematic representation. a Top view and b front view of the optimized system of the possible interactions between Acid Red 337 and the mesoporous silica, calculated by using DFT//B97D3/6-31G(d) level of theory

initial geometries of the dye and the MS were constructed using the graphical interface ChemOffice 3D ultra (Evans and Rubenstein 2012). The isolated molecules are subsequently subjected to energy minimization separately in the gas phase with tight convergence criteria without imposing any geometrical or symmetrical restrictions, using the density functional theory (DFT) (Hohenberg and Kohn 1964) by applying the exchange-correlation functional B97D3 combined with 6–31 g (Binkley et al. 1980) basis sets implemented in G09 (Glendening et al. 2009). The B97D3 functional uses the latest D3 version (Antony and Grimme 2006; Grimme et al. 2010, 2011) developed by Grimme that included the dispersion correction term, which provided a reasonably accurate description of the no covalent interactions, specifically the weak interactions as the hydrogen bonding and the Van Der Waals interactions. To evaluate the optimized structures of stationary points, corresponding to true minima, the harmonic frequency calculations have been performed at the same level of the theory (are a very important feature indicating that all frequencies are real).

In the second step of this work, the obtained results from the optimized structures are used as input in the optimized system, and the calculation of the binding energies or so-called the complexation energies ΔE which carried out to explain the interaction exists be- tween adsorbate and adsorbent. These energies were evaluated in the framework of the supermolecular (SM) approach proposed by Boys and Bernardi (1970) and Simon et al. (1996), which is known as a counter- poise correction (CP); it is calculated according to the following equation:

$$\Delta E = E_{System} - (E_{RED} - A) + E_{SI} + BSSE \quad (4)$$

where ΔE in Eq. (4) represents the binding energies of the complex, corresponding to the difference between the total energies of complex and the two isolated monomers of the free Acid Red 337 and MS, respectively, with the consideration of the effects on the basis set superposition error (BSSE) (Jansen and Ros 1969; Liu and McLean 1973) to correct the bond- ing energy.

Theoretical results are presented in Fig. 13, which allows the identification of reactive sites explaining the formation of the H bonds in the complex. The chemical bond is formed between the hydrogen atoms of the Acid Red 337 dye molecule and the surface hydroxyl groups of MS. However, the calculated bonding energy is negative suggesting a strong interaction between ad- sorbate and adsorbent molecules. The results reveal that the energy of this interaction using the counterpoise theory is − 81.65 kcal/mol.

Conclusions

This study determined that mesoporous silica was successfully synthesized from local raw clay (DD3) of Guelma province in Algeria as a source of silica. Before its use, the clay underwent two treatments: thermal and chemical. In addition, the Pluronic L35 has been used as a structuring agent.

Several characterization analyses were used to evaluate the textural and structural properties as well as the composition of the synthesized material. Mesoporous silica gives a surface area of 161 m^2/g which shows promising results of adsorption to Acid Red 337 dyes in aqueous solutions.

In addition, it was noted that pH is the most important factor to affect the dye removal and it was found that the interaction between the dye and the surface of MS could be explained by H bonding.

Acknowledgments This work was done in the frame of the ERANETMED SETPROpER project "Sustainable textile effluent treatment processes of reuse of water in agriculture" (2016–2019) with the support of the funding agency of Algeria (DGRSDT).

The authors would like to gratefully acknowledge Mrs. Rabia Gueraiche (engineer in the COTITEX company) for providing the reel effluent textile.

References

Aber S, Sheydaei M (2012) Removal of COD from industrial effluent containing indigo dye using adsorption method by activated carbon cloth: optimization, kinetic, and isotherm studies. Clean Soil Air Water 40(1):87–94. https://doi.org/10.1002/clen.201000434

Acisli O, Khataee A, Karaca S, Sheydaei M (2016) Modification of nanosized natural montmorillonite for ultrasound-enhanced adsorption of Acid Red 17. Ultrason Sonochem 31:116–121. https://doi.org/10.1016/j.ultsonch.2015.12.012

Aguayo-Villarreal IA, Hernández-Montoya V, Rangel-Vázquez NA, Montes-Morán MA (2014) Determination of QSAR properties of textile dyes and their adsorption on novel carbonaceous adsorbents. J Mol Liq 196:326–333. https://doi.org/10.1016/j.molliq.2014.04.008

Ahmad AA, Hameed BH (2009) Reduction of COD and color of dyeing effluent from a cotton textile mill by adsorption onto bamboo-based activated carbon. J Hazard Mater 172:1538–1543. https://doi.org/10.1016/j.jhazmat.2009.08.025

Ahmed MJ (2016) Application of agricultural based activated carbons by microwave and conventional activations for basic dye adsorption: review. J Environ Chem Eng 4:89–99. https://doi.org/10.1016/j.jece.2015.10.027

Antony J, Grimme S (2006) Density functional theory including dispersion corrections for intermolecular interactions in a large benchmark set of biologically relevant molecules. Phys Chem Chem Phys 8:5287–5293. https://doi.org/10.1039/b612585a

APHA (1998) Standard methods for the examination of water and wastewater, 20th edn. American Public Health Association, Washington, DC

Atrous M, Sellaoui L, Bouzid M, Lima EC, Thue PS, Bonilla-Petriciolet A, Ben Lamine A (2019) Adsorption of dyes acid red 1 and acid green 25 on grafted clay: modeling and statistical physics interpretation. J Mol Liq 294:111610. https://doi.org/10.1016/j.molliq.2019.111610

Auta M, Hameed BH (2012) Modified mesoporous clay adsorbent for adsorption isotherm and kinetics of methylene blue. Chem Eng J 198–199:219–227. https://doi.org/10.1016/j.cej.2012.05.075

Baskaran T, Christopher J, Ajithkumar TG, Sakthivel A (2014) SBA-15 intercalated Mg–Al hydrotalcite: an environmental friendly catalyst for hydroisomerization of olefin. Appl Catal A Gen 488:119–127. https://doi.org/10.1016/j.apcata.2014.09.024

Bhuiyan TI, Arudra P, Akhtar MN, Aitani AM, Abudawoud RH, Al-Yami MA, Al-Khattaf SS (2013) Metathesis of 2-butene to propylene over W-mesoporous molecular sieves: a comparative study between tungsten containing MCM-41 and SBA-15. Appl Catal A Gen 467:224–234. https://doi.org/10.1016/j.apcata.2013.07.034

Binkley JS, Pople JA, Hehre WJ (1980) Self-consistent Molecular Orbital Methods 21. Small split-valence basis sets for first-row elements. J Am Chem Soc 102(3):939–947. https://doi.org/10.1021/ja00523a008

Boys SF, Bernardi F (1970) The calculation of small molecular interactions by the differences of separate total energies. Some procedures with reduced errors. Mol Phys 19(4):553–566. https://doi.org/10.1080/00268977000101561

Bui VKH, Park D, Pham TN, An Y, Choi JS, Lee H-U, Kwon O-H, Moon J-Y, Kim K-T, Lee Y-C (2019) Synthesis of MgAC-Fe3O4/TiO2 hybrid nanocomposites via sol-gel chemistry for water treatment by photo-Fenton and photocatalytic reactions. Sci Rep 9:1–11. https://doi.org/10.1038/s41598-019-48398-5

Chaudhuri H, Dash S, Sarkar A (2015) Synthesis and use of SBA-15 adsorbent for dye-loaded wastewater treatment. J Environ Chem Eng 3:2866–2874. https://doi.org/10.1016/j.jece.2015.10.009

Chaudhuri H, Dash S, Sarkar A (2016) SBA-15 functionalised with high loading of amino or carboxylate groups as selective adsorbent for enhanced removal of toxic dyes from aqueous. New J Chem 15. https://doi.org/10.1039/C5NJ02816G

Chen C, You KS, Ahn JW, Ahn WS (2010) Synthesis of mesoporous silica from bottom ash and its application for CO2 sorption. Korean J Chem Eng 27(3):1010–1014. https://doi.org/10.1007/s11814-010-0153-3

Du C, Yang H (2012) Investigation of the physicochemical aspects from natural kaolin to Al-MCM-41 mesoporous materials. J Colloid Interface Sci 369:216–222. https://doi.org/10.1016/j.jcis.2011.12.041

Eftekhari S, Habibi-Yangjeh A, Sohrabnezhad SH (2010) Application of AlMCM-41 for competitive adsorption of methylene blue and rhodamine B: thermodynamic and kinetic studies. J Hazard Mater 178:349–355. https://doi.org/10.1016/j.jhazmat.2010.01.086

Elmoubarki R, Mahjoubi FZ, Tounsadi H, Moustadraf J, Abdennouri M, Zouhri A, El Albani A, Barka N (2015) Adsorption of textile dyes on raw and decanted Moroccan clays: kinetics, equilibrium and thermodynamics. Water Resour Ind 9:16–29. https://doi.org/10.1016/j.wri.2014.11.001

Evans DA, Rubenstein S (2012) Reference of using the graphical interface Chem-Office 3D ultra (ChemDraw™ Professional 12.0). http://www.cambridgesoft.com

Fardjaoui N, Zohra F, Berrichi E, Ayari F (2017) Kaolin-issued zeolite A as efficient adsorbent for Bezanyl Yellow and Nylomine Green anionic dyes. Microporous Mesoporous Mater 243:91–101. https://doi.org/10.1016/j.micromeso.2017.01.008

Frost RAYL, Vassallo AM (1996) The dehydroxylation of the kaolinite clay minerals using infrared emission spectroscopy. Clay Clay Miner 44:635–651

Georgin J, Alves E, Drumm F, Tonato D, Grassi P, Piccin JS, Oliveira MLS, Dotto GL, Mazutti MA (2019) Application of Beauveria bassiana spore waste as adsorbent to uptake acid red 97 dye from aqueous medium. Environ Sci Pollut Res 26(36):36967–36977. https://doi.org/10.1007/s11356-019-06792-6

Ghaly A, Ananthashankar R, Alhattab M, Ramakrishnan V (2014) Production, characterization and treatment of textile effluents: a critical review. J Chem Eng Process Technol 2014(05):1–19. https://doi.org/10.4172/2157-7048.1000182

Glendening ED, Reed AE, Carpenter JE, Weinhold F (2009) NBO Version 3.1, Frisch. M.J et al. Gaussian 09 Revision E.01. Gaussian Inc, Wallingford CT NBO Version 3.1, E. D. Glendening, A. E. Reed, J. E. Carpenter, and F. Weinhold

Gómez JM, Galán J, Rodríguez A, Walker GM (2014) Dye adsorption onto mesoporous materials: pH influence, kinetics and equilibrium in buffered and saline media. J Environ Manag 146:355–361. https://doi.org/10.1016/j.jenvman.2014.07.041

Grimme S, Antony J, Ehrlich S, Krieg H (2010) A consistent and accurate ab initio parametrization of density functional dispersion correction (DFT-D) for the 94 elements H-Pu. J Chem Phys 132. https://doi.org/10.1063/1.3382344

Grimme S, Ehrlich S, Goerigk L (2011) Effect of the damping function in dispersion corrected density functional theory. Comput Chem 32:1456–1465. https://doi.org/10.1002/jcc

Guesh K, Mayoral Á, Márquez-Álvarez C, Chebude Y, Díaz I (2016) Enhanced photocatalytic activity of TiO2 supported on zeolites tested in real wastewaters from the textile industry of Ethiopia. Microporous Mesoporous Mater 225:88–97. https://doi.org/10.1016/j.micromeso.2015.12.001

Hohenberg P, Kohn W (1964) Inhomogeneous Electron Gas. Phys Rev B 136:864–871. https://doi.org/10.1103/PhysRev.136.B864

ISO 10523 (2008) Date de publication: 2008-12. URL: iso.org/fr/standard/51994.html

Jansen HB, Ros P (1969) Non-Empirical molecular orbital calculations on the protonation of carbon monoxide. Chem Phys Lett 3:140–143. https://doi.org/10.1016/0009-2614(69)80118-1

Khan TA, Khan EA, Shahjahan (2015) Removal of basic dyes from aqueous solution by adsorption onto binary iron-manganese oxide coated kaolinite: non-linear isotherm and kinetics modeling. Appl Clay Sci 107:70–77. https://doi.org/10.1016/j.clay.2015.01.005

Khattri SD, Singh MK (2009) Removal of malachite green from dye wastewater using neem sawdust by adsorption. J Hazard Mater 167:1089–1094. https://doi.org/10.1016/j.jhazmat.2009.01.101

Kim TW, Kleitz F, Paul B, Ryoo R (2005) MCM-48-like large mesoporous silicas with tailored pore structure: facile synthesis domain in a ternary triblock copolymer-butanol-water system. J Am Chem Soc 127:7601–7610. https://doi.org/10.1021/ja042601m

Li X, Li B, Xu J, Wang Q, Pang X, Gao X, Zhou Z, Piao J (2010) Synthesis and characterization of Ln-ZSM-5/MCM-41 (Ln = La, Ce) by using kaolin as raw material. Appl Clay Sci 50:81–86. https://doi.org/10.1016/j.clay.2010.07.006

Li T, Shu Z, Zhou J, Chen Y, Yu D, Yuan X, Wang Y (2015) Template-free synthesis of kaolin-based mesoporous silica with improved specific surface area by a novel approach. Appl Clay Sci 107:182–187. https://doi.org/10.1016/j.clay.2015.01.022

Li Q, Zhang J, Lu Q, Lu J, Li J, Dong C, Zhu Q (2016) Hydrothermal synthesis and characterization of ordered mesoporous magnesium silicate-silica for dyes adsorption. Mater Lett 170:167–170. https://doi.org/10.1016/j.matlet.2016.02.029

Liu B, McLean A (1973) Accurate calculation of the attractive interaction of two ground state helium atoms. J Chem Phys 59(8):4557. https://doi.org/10.1063/1.1680654

Madhusoodana CD, Kameshima Y, Nakajima A, Okada K (2006) Synthesis of high surface area Al-containing mesoporous silica from calcined and acid leached kaolinites as the precursors. J Colloid Interface Sci 297:724–731. https://doi.org/10.1016/j.jcis.2005.10.051

Mellouk S, Cherifi S, Sassi M, Marouf-Khelifa K, Bengueddach A, Schott J, Khelifa A (2009) Intercalation of halloysite from Djebel Debagh (Algeria) and adsorption of copper ions. Appl Clay Sci 44: 230–236. https://doi.org/10.1016/j.clay.2009.02.008

Mureseanu M, Cioatera N, Trandafir I, Georgescu I, Fajula F, Galarneau A (2011) Selective Cu 2 + adsorption and recovery from contaminated water using mesoporous hybrid silica bio-adsorbents. Microporous Mesoporous Mater 146:141–150. https://doi.org/10.1016/j.micromeso.2011.04.026

NCASI Method 71.01 (1999) Color measurement in pulp mill wastewater by spectrophotometry method. NCASI, USA

Pan F, Lu X, Wang T, Wang Y, Zhang Z, Yan Y (2013) Triton X-100 directed synthesis of mesoporous γ -Al 2 O 3 from coal-series kaolin. Appl Clay Sci 85:31–38. https://doi.org/10.1016/j.clay.2013.09.007

Pang X, Tang F (2005) Morphological control of mesoporous materials using inexpensive silica sources. Microporous Mesoporous Mater 85:1–6. https://doi.org/10.1016/j.micromeso.2005.06.012

Qoniah I, Prasetyoko D, Bahruji H, Triwahyono S, Abdul A, Esti T (2015) Direct synthesis of mesoporous aluminosilicates from Indonesian kaolin clay without calcination. Appl Clay Sci 118: 290–294. https://doi.org/10.1016/j.clay.2015.10.007

Santos SCR, Oliveira ÁFM, Boaventura RAR (2015) Bentonitic clay as adsorbent for the decolourisation of dyehouse effluents. J Clean Prod 126:667–676. https://doi.org/10.1016/j.jclepro.2016.03.092

Sheng L, Zhang Y, Tang F, Liu S (2017) Preparation from natural sands and highly efficient fixed-bed adsorption of methylene blue in waste water. Microporous Mesoporous Mater 257:9–18. https://doi.org/10.1016/j.micromeso.2017.08.023

Shukla A, Zhang Y, Dubey P, Margrave JL, Shukla SS (2002) The role of sawdust in the removal of unwanted materials from water. J Hazard Mater 95(2002):137–152

Simon S, Duran M, Dannenberg JJ (1996) How does basis set superposition error change the potential surfaces for hydrogenbonded dimers? J Chem Phys 105:11024. https://doi.org/10.1063/1.472902

Sing KS Wet al (1985) Reporting physisorption data for gas/solid systems with special reference to the determination of surface area and porosity (recommendations 1984). Pure Appl Chem 57:603–619. https://doi.org/10.1351/pac198557040603

Tanev PT, Pinnavaia TJ (1996) Mesoporous silica molecular sieves prepared by ionic and neutral surfactant templating: a comparison of physical properties. Chem Mater 8(8):2068–2079. https://doi.org/10.1021/cm950549a

Thue PS, Sophia AC, Lima EC, Wamba AGN, de Alencar WS, dos Reis GS, Rodembusch FS, Dias SLP (2018) Synthesis and characterization of a novel organic-inorganic hybrid clay adsorbent for the removal of acid red 1 and acid green 25 from aqueous solutions. J Clean Prod 171:30–44. https://doi.org/10.1016/j.jclepro.2017.09.278

Tsai C, Chang W, Saikia D, Wu C, Kao H (2015) Functionalization of cubic mesoporous silica SBA-16 with carboxylic acid via one-pot synthesis route for effective removal of cationic dyes. J Hazard Mater 309:236–248. https://doi.org/10.1016/j.jhazmat.2015.08.051

Verma AK, Dash RR, Bhunia P (2012) A review on chemical coagulation / flocculation technologies for removal of colour from textile wastewaters. J Environ Manag 93:154–168. https://doi.org/10.1016/j.jenvman.2011.09.012

Xin G, Wang M, Chen L, Zhang Y, Wang M (2019) Synthesis and properties of zeolite / N-doped porous carbon for the e ffi cient removal of chemical oxygen demand and ammonia-nitrogen from aqueous solution. RSC Adv:6452–6459. https://doi.org/10.1039/c8ra08800d

Yagub MT, Sen TK, Afroze S, Ang HM (2014) Dye and its removal from aqueous solution by adsorption: a review. Adv Colloid Interf Sci 209:172–184. https://doi.org/10.1016/j.cis.2014.04.002

Yan L, Qin L, Yu H, Li S, Shan R, Du B (2015) Adsorption of acid dyes from aqueous solution by CTMAB modified bentonite: kinetic and isotherm modeling. J Mol Liq 211:1074–1081. https://doi.org/10.1016/j.molliq.2015.08.032

Yang N, Zhu S, Zhang D, Xu S (2008) Synthesis and properties of magnetic Fe 3 O 4 -activated carbon nanocomposite particles for dye removal. Mater Lett 62:645–647. https://doi.org/10.1016/j.matlet.2007.06.049

Zhang X, Zheng X, Zhang S, Zhao B, Wu W (2012) AM-TEPA impregnated disordered mesoporous silica as CO2 capture adsorbent for balanced adsorption-desorption properties. Ind Eng Chem Res 51(46):15163–15169. https://doi.org/10.1021/ie300180u

Zhang X, Zhang S, Qin H, Wu W (2014) Development of TRPN dendrimer-modified disordered mesoporous silica for CO_2 capture. Mater Res Bull 56:12–18. https://doi.org/10.1016/j.materresbull.2014.04.041

Zhang F, Sun C, Li S, Yang L, Chao X (2015) Synthesis of SBA-15 using natural clay from low-grade potash ores of a salt lake in Qinghai, China. Adv Comput Sci Res 33. https://doi.org/10.2991/iwmecs-15.2015.110

Zhao D, Feng J, Huo Q, Melosh N, Glenn H, Chmelka BF, Stucky GD, Melosh N, Fredrickson GH, Chmelka BF, Stucky GD (1998) Triblock copolymer syntheses of mesoporous silica with periodic 50 to 300 angstrom pores. Science 279(5350):548–552

Zhou C, Sun T, Gao Q, Alshameri A, Zhu P (2013) Synthesis and characterization of ordered mesoporous aluminosilicate molecular sieve from natural halloysite. J Taiwan Inst Chem Eng 45:1073–1079. https://doi.org/10.1016/j.jtice.2013.09.030